Immunogenic Potential of a Multi-Peptide Vaccine Construct Against Uropathogenic *Escherichia coli*-Associated Urinary Tract Infection

Saeide Mirsharifi¹, Mehri Habibi², Touraj Rahimi^{3,4}, Fatemeh Foroohi^{1*}, Mohammad Reza Asadi Karam^{5*}

¹Department of Microbiology, ShQ.C., Islamic Azad University, Shahr-e Qods, Iran;
²Biotechnology Department, Biotechnology Research Center, Pasteur Institute of Iran, Pasteur Ave.,
Tehran 1316943551, Iran;
³Department of Plant Production and Genetics, ShQ.C., Islamic Azad University,
Shahr-e Qods, Iran;
⁴Research Center for Medicinal Plants, ShQ.C., Islamic Azad University, Shahr-e Qods, Iran;
⁵Department of Molecular Biology, Pasteur Institute of Iran, Pasteur Ave., Tehran 1316943551, Iran

OPEN ACCESS

Article type: Research Article Received: August 4, 2025 Revised: June 21, 2025 Accepted: June 28, 2025 Published online: June 30, 2025

How to cite:

Mirsharifi S, Habibi M, Rahimi T, Foroohi F, Asadi Karam MR. Immunogenic Potential of a Multi-Peptide Vaccine Construct Against Uropathogenic Escherichia coli-Associated Urinary Tract Infection. Iran. Biomed. J. 2025; 29(4): 247-259.



This article is licensed under a Creative Commons Attribution-NonDerivatives 4.0 International

ABSTRACT

Background: Urinary tract infection caused by UPEC is a common infectious disease. The growing frequency of antibiotic resistance highlights the need for alternative strategies, such as vaccines, to combat UTIs. This study aimed to evaluate the immunogenicity of a novel vaccine candidate targeting UPEC.

Methods: Different bioinformatics servers were used to design a vaccine candidate composed of PapG II and FimH antigens from UPEC, along with the N- (1-173) and C-terminal (401-495) domains of FliC from *S. typhimurium*. The final construct was cloned into the pET28a vector, expressed, purified, and confirmed using SDS-PAGE and Western blotting. Mice were immunized with the recombinant protein, both with and without alum adjuvant, and antibody responses were measured using ELISA.

Results: The final vaccine construct included one domain of PapG II (81 aa) and FimH (83 aa). The conserved domains of FliC were incorporated into the construct. SDS-PAGE and Western blot confirmed the purification of the protein, with a size of 53 kDa. Immunization of mice with PapG.FimH.FliC protein induced significantly higher levels of serum IgG, IgG isotypes, IgA, as well as mucosal IgA and IgG responses compared to the controls (p < 0.05). The addition of alum to the protein significantly enhanced serum IgG1 and IgA and mucosal IgG, compared to the protein without alum (p < 0.05).

Conclusion: The vaccine construct induced significant humoral responses in the mouse model, suggesting its potential as a promising candidate against UPEC. However, additional experimental analyses are required to validate the efficacy of the vaccine construct. **DOI:** 10.61186/ibj.5149

Keywords: Flagellin, Urinary tract infections, Uropathogenic Escherichia coli, Vaccines

Corresponding Authors:

Fatemeh Foroohi

Department of Microbiology, ShQ.C., Islamic Azad University, Shahr-e Qods, Iran; E-mail: drforoohi@iau.ac.ir; ORCID ID: 0000-0003-1816-0689

Mohammad Reza Asadi Karam

Department of Molecular Biology, Pasteur Institute of Iran, Tehran, Iran. Email: m_asadi12@yahoo.com; ORCID ID: 0000-0003-1000-9116

List of Abbreviations:

2D: two-dimensional; **3D:** three-dimensional; **C-score:** confidence score; *E. coli:* Escherichia coli; ELISA: enzyme-linked immunosorbent assay; **FliC:** flagellin; **GRAVY:** grand average of hydropathicity; **IEDB:** Immune epitope database; **LB:** Luria bertani; **LPS:** lipopolysaccharide; **Pap:** pyelonephritis-associated pili; **pl:** isoelectric point; *S. typhimurium:* Salmonella typhimurium; **TLR:** toll-like receptor; **TMB:** 3,3′,5,5′-tetramethylbenzidine; **UPEC:** uropathogenic *E. coli*; **UTI:** urinary tract infection; **VF:** virulence factor

INTRODUCTION

Trinary tract infection is recognized as the second common infectious disease in humans. Its high prevalence, along with the increasing frequency of antibiotic resistance among UTI-causing pathogens, highlights the need for alternative strategies to manage these infections. *E. coli* strains are the main cause of all types of UTIs, and most research has focused on these strains^[1].

UPEC presents various VFs that facilitate colonization and invasion of the host tissues. Key VFs include adhesions, siderophores, toxins, surface polysaccharides, and outer membrane proteins^[2]. Among them, adhesions have a wide diversity among different UPEC classes. P fimbriae are among the most important adhesions, mediating UPEC binding to host surfaces through PapG subunit. The Pap gene cluster, composed of 11 genes, encodes papA, papEF, and the adhesion gene papG. PapG exists in four molecular variants (I-IV), each with distinct receptor-binding properties that may influence host specificity and clinical manifestations of UTI^[3]. Type 1 pili are another colonization factor in UPEC, enabling the attachment of oligomannose-containing the strains to the glycoproteins on the human bladder. The FimH adhesion, located on type 1 pili, plays a critical role in mediating the colonization, invasion, and formation of intracellular reservoirs by UPEC in the bladder^[4]. Studies have indicated that, similar to LPS, FimH acts as a ligand for TLR-4 and can stimulate the immune system, making it a potential innate adjuvant for vaccine development^[5,6].

Subunit vaccines, which utilize proteins or peptides, often exhibit low immunogenicity and require effective adjuvants to elicit robust and long-lasting immune responses^[7,8]. FliC, the major structural protein of flagella in motile bacteria, activates innate immune responses by recognizing TLR-5 on immune cells, hence stimulating acquired immunity. Therefore, the FliC of bacteria, especially FliC from *S. typhimurium*, has been applied as a vaccine adjuvant in different studies^[9].

Previous research has shown that type 1 and P fimbriae are essential for bladder colonization and ascension of UPEC into the kidneys, respectively^[10]. Therefore, incorporating FimH and PapG adhesions from type 1 and P pili into a single vaccine construct, may offer protection against both cystitis and pyelonephritis caused by UPEC in the host.

In the present study, we aimed to design a novel vaccine construct composed of the PapG and FimH antigens from the UPEC strain, as well as the FliC from *S. typhimurium* strain as an innate adjuvant. The vaccine construct was designed using bioinformatics and

immunoinformatics techniques, expressed in a prokaryotic system and evaluated for its ability to induce humoral immune responses in a mouse model.

MATERIALS AND METHODS

Extraction of protein sequence

The protein sequences of PapG II (UniProt: O86476-1) and FimH (UniProt: P08191) from *E. coli* subsp. CFT073, as well as FliC (UniProt: P06179) from *S. typhimurium*, were extracted from the Uniprot database (https://www.uniprot.org/)^[11]. For further analysis, we focused on residues 22-174 of the FimH protein sequence, which correspond to the binding (lectin) domain^[12], and residues 21-226 of PapG II, representing the carbohydrate-binding domain^[13]. Also, we selected the D0 and D1 domains of FliC, comprising residues 1-173 from the N-terminal region and residues 401-495 from the C-terminal region.

Prediction of B-lymphocyte epitopes

To identify the potential B-cell epitopes within the PapG II and FimH protein sequences, three different servers were used: ABCpred (http://www.imtech.res.in/raghava/abcpred), BCpred (http://ailab.ist.psu.edu/bcpred/), and IEDB (http://tools.immuneepitope.org/bcell/). The regions identified as epitopes by all three servers, were selected for further analysis. These selected B-cell epitopes were then evaluated for their antigenicity using VaxiJen v2.0 (http://www.ddgpharmfac.net/vaxiJen/VaxiJen/VaxiJen.html)^[14].

Prediction of T-cell epitopes

T-cell epitopes were predicted using TepiTool (http://tools.iedb.org/tepitool/)^[15]. For MHC-I epitope prediction, we fixed the peptide length to 9mer, which is the preferred length for ligand binding to HLA alleles. We also selected 27 of the most frequent human HLA-A and HLA-B alleles, as well as mouse alleles H-2-Dd, H-2-Kd, and H-2-Ld, for the analysis of MHC-I binding epitopes with percentile rank ≤1. For predicting MHC-II binding epitopes (15mer), we selected all human DR alleles including DRB1*01:01, DRB1*03:01, DRB1*04:01, DRB1*04:05, DRB1*07:01, DRB1*08:02, DRB1*09:01, DRB1*11:01, DRB1*12:01, DRB1*13:02, DRB1*15:01, DRB3*01:01, DRB3*02:02, DRB4*01:01, DRB5*01:01 and mouse alleles (H2-IAd and H2-IEd) with percentile rank ≤ 10 .

Evaluation of the vaccine construct

The physicochemical properties of the vaccine construct were analyzed using the Expasy Protparam online server (https://web.expasy.org/protparam/)^[16].

The antigenicity of the vaccine was assessed using VaxiJen 2.0. For screening allergenicity, we used the (https://www.ddg-AllerTop v2.0server pharmfac.net/AllerTOP/method.html)[17], while toxicity screening was performed using **ToxinPred** (https://webs.iiitd.edu.in/raghava/toxinpred/algo.php)[1] 8]. Additionally, we predicted protein solubility upon overexpression in E. coli using the Protein-sol server (https://protein-sol.manchester.ac.uk/)^[19].

Prediction of the secondary structure

To predict the secondary structure of the vaccine construct, we employed the Garnier-Osguthorpe Robson IV server (https://npsa-prabi.ibcp.fr/cgibin/npsa_automat.pl?page=/NPSA/npsa_gor4.html)^[20]. In this analysis, we input the amino acid sequence of the construct to determine its secondary protein structure.

Prediction of the tertiary structure of the vaccine construct

The tertiary structure of the vaccine construct was predicted using the I-TASSER (https://zhanggroup.org/I-TASSER/)^[21]. This server computes the C-score to assess the quality of the predicted models. The selected 3D model was then refined using the GalaxyRefine server (https://galaxy.seoklab.org/cgi-bin/submit.cgi? type =REFINE) to improve its structural quality^[22]. The Discovery Studio visualizer was employed to visualize the 3D models. The overall quality of the protein structure was evaluated using the Z-score generated by ProSA-web (https://prosa.services.came.sbg.ac.at/prosa.php)^[23]. Additionally, the Ramachandran plot was created using the SAVES v6.0 PROCHECK tool (https://saves.mbi.ucla.edu/)^[24].

Molecular docking of the vaccine construct with TLRs

The binding ability of the vaccine construct to TLR-5 and TLR-4 was evaluated through molecular docking, using the Cluspro 2.0 server (http://cluspro.bu.edu/login.php)^[25]. The PDB files for TLR-5 (PDB ID: 3J0A) and TLR-4 (PDB ID: 3FXI) were obtained from the RCSB PDB website (https://www.rcsb.org/). The results obtained from Cluspro 2.0 were further analyzed using PRODIGY (https://nestor.science.uu.nl/prodigy/) to find the binding affinity (kcal/mol) and the dissociation constant (Kd) (M) of the docked vaccine construct-TLR complex^[26]. The Discovery Studio visualizer was employed to visualize the docking complexes. Furthermore, PDBsum was used to identify and map the interacting residues between the vaccine construct and TLRs^[27].

In silico evaluation of immune response

To evaluate the potential immune response of the vaccine construct, we performed in silico immune simulations using the C-ImmSim online server (https://kraken.iac.rm.cnr.it/C-IMMSIM/)^[28]. In the simulation step, we administered three injections at time points 1, 84, and 168 (one time step corresponds to 8 h in real life). All other parameters were at their default values.

Expression and purification of the recombinant protein

The codon-optimized gene construct was synthesized by Biomatik Company (Canada) and subsequently cloned into the pET28a vector. The recombinant vector was transformed into the competent E. coli BL21 (DE3) cells, which were cultured on LB agar plates overnight. Colonies containing the recombinant plasmid were confirmed through double digestion with NcoI and HindIII enzymes, followed by sequencing. For protein expression, the bacteria were cultured in LB broth medium, and protein expression was induced by IPTG. The bacterial cells were harvested by centrifugation and analyzed by SDS-PAGE. The protein bands were confirmed using Western blotting with anti-His tag monoclonal antibody (Sigma, USA). The recombinant protein was purified using Ni-NTA affinity chromatography (Qiagen, USA)^[29]. A commercial LPS removal kit (Thermo Fisher Scientific, Lithuania) was employed to remove LPS contamination from the recombinant protein. Finally, the purified protein was dialyzed and quantified by the BCA assay kit (DNAbiotech, Iran).

Immunization of mice

Female BALB/C mice (6-8 weeks) were purchased from the Pasteur Institute of Iran (Tehran). The mice were housed in a room with a temperature of 20-22 °C and humidity levels of 50-60%. They were provided with standard rodent chow, which had access to water ad libitum. The mice were randomly divided into four groups (n = 10/group). Group 1 was vaccinated with the recombinant protein alone (30 µg), group 2 was given the recombinant protein combined with aluminum hydroxide (alum) adjuvant (30 µg of protein + 200 µg of alum), group 3 received alum alone (200 µg), and group 4 was administered PBS alone. All vaccine formulations were administered subcutaneously in a total volume of 100 µl on days 0, 14, and 28. Sera and urine samples were collected from each group 14 days after the last vaccine dose to measure antibody levels.

Antibody assay test

ELISA was used to evaluate the antibody responses specific to the recombinant protein in serum and urine samples collected from the mice. Briefly, purified protein (10 $\mu g/ml$) was coated onto microtiter plates (Greiner, Germany). Following overnight incubation, the plates were washed several times, and the sera (diluted from 1:100 to 1:64500) or urine (diluted from 1:2 to 1:50) were added. After antigen-antibody binding, the plates were washed and incubated with horseradish peroxidase-conjugated rabbit anti-mouse antibody (Sigma, USA). The plates were washed again, and the TMB substrate was added to the plates. The reaction was stopped after 20 min, and OD was measured at 450 $\rm nm^{[30]}$.

Statistical analysis

A statistical analysis of the immune responses was carried out using one-way analysis of variance (ANOVA), followed by Student's t-test and Tukey's HSD tests. GraphPad Prism software (version 6.0) was used to generate the figures illustrating immune responses. In the experiments, p values <0.05 were considered statistically significant.

RESULTS

Retrieval and alignment of protein sequences

In this study, the protein sequences of PapG II and FimH were obtained from the UniProt database to create a vaccine construct targeting UPEC strains. The alignment of these protein sequences showed identities of over 97.9% for PapG II and 98.7% for FimH among *E. coli* strains, indicating that these proteins are conserved.

Prediction of linear B-cell epitope

The mature sequences of the PapG II and FimH were evaluated using ABCpred, BCPred, and BepiPred v2.0. Epitopes were selected based on high prediction scores and overlapping results from the three online servers. The analysis identified one region in each protein with the highest linear B-cell epitopes. The overlapping results of the predicted linear B-cell epitopes from the three servers are shown in Table 1. The regions comprising amino acids 46 to 128 of the lectin domain of FimH (NDYPETITDYVTLQRGAAYGGVLSSF SGTVKYNGSSYPFPTTSETPRVVYNSRTDKPWPV AL YLTPVSSAGGVAIKAGSLIAV) with the highest number of B-cell epitopes were selected. There were seven B-cell epitopes for FimH in the selected region. VaxiJen score for the region was 0.43, exceeding the threshold score (0.4). In addition, amino acids 70 to 150 of the carbohydrate-binding domain of PapG II (VMTQNGYPLFIEVHNKGSWSEENTGDNDSYFFL KGYKWDERAFDTANLCQKPGEKTRLTEKFDDII FKVALPADLPLGDYS) with seven B-cell epitopes and a vaxiJen score of 0.53 were selected.

Prediction of T-cell epitopes of proteins

The prediction of T-cell epitopes was conducted for selected regions of PapG II (amino acids 70-150) and FimH (amino acids 46-128) using the IEDB Tepitool server. The results showed that peptide fragments from each antigen contained several T-cell epitopes for different human and mouse MHC-I and MHC-II alleles. For the selected regions of FimH, the TepiTool server predicted 29 and 10 epitopes (9mer) for human and BALB/c H-2 MHC I alleles, respectively. Overall, 18 epitopes were identified for PapG II that interacted with 23 MHC-I alleles, along with six epitopes predicted for BALB/c H-2 class I (Table 2).

Table 1. The overlapped results of the predicted linear B-cell epitopes from three servers

Protein	Linear B-cell epitope	Sever	Antigenicity (cut off ≥ 0.4)
	KGSWSEENTGDNDSYF	ABCpred	0.50
	VMTQNGYPLFIEVHNK	ABCpred	0.48
PapG II	GEKTRLTEKFDDIIFK	ABCpred	0.99
	NKGSWSEENTGDNDSY	Bepred	0.69
	FLKGYKWDERAFDTAN	Bcpred	0.27
	KWDERAFDTANLCQKPGEKTRLTEKF	IEDB	0.81
	KGSWSEENTGDND	IEDB	0.95
	When the thin W.W.N.C.	A D.C., d	0.40
	YPFPTTSETPRVVYNS	ABCpred	0.49
	PETITDYVTLQRGAAY	ABCpred	0.10
FimH	SGTVKYNGSSYPFPTT	ABCpred	0.40
	YNSRTDKPWPVALYLT	ABCpred	0.76
	PFPTTSETPRVVYNSR	Bcpred	0.41
	SSYPFPTTSETPRVVYNSRTDKP	IEDB	0.49
	QRGAAYGGVLSSFS	IEDB	0.20

Table 2. MHC-I binding epitopes predicted by the TepiTool server with antigenicity score exceeding the threshold value

Protein	Epitope	No. of human MHC-I alleles	Antigenicity (cut off ≥ 0.4)	Epitope	No. of mouse MHC-I alleles	Antigenicity
	sequence			sequence		
	MTQNGYPLF	10	Non-antigen	VMTQNGYP	H-2-Kd	Non-antigen
	TQNGYPLFI	4	0.74	L	H-2-Dd	Non-antigen
	NGYPLFIEV	3	0.70	MTQNGYPL	H-2-Dd	0.74
	IEVHNKGSW	2	Non-antigen	F	H-2-Dd, H-2-Ld	0.70
	NTGDNDSYF	2	0.50	TQNGYPLFI	H-2-Kd	1.26
	TGDNDSYFF	1	Non-antigen	NGYPLFIEV	H-2-Ld	0.91
D 0.77	GDNDSYFFL	1	Non-antigen	KFDDIIFKV		
PapG II	DSYFFLKGY	3	Non-antigen	VALPADLPL		
(70-150)	SYFFLKGYK	3	Non-antigen			
	YFFLKGYKW	6	0.5			
	GYKWDERAF	2	0.77			
	CQKPGEKTR	1	1.66			
	KPGEKTRLT	1	1.41			
	TEKFDDIIF	3	0.4			
	KFDDIIFKV	5	1.26			
	DDIIFKVAL	1	0.87			
	VALPADLPL	2	0.91			
	PADLPLGDY	1	Non-antigen			
	DYPETITDY	2	Non-antigen	YPETITDYV	H-2-Ld	Non-antigen
	YPETITDYV	3	Non-antigen	RGAAYGGV	H-2-Dd	Non-antigen
	ETITDYVTL	2	Non-antigen	L	H-2-Kd	Non-antigen
	ITDYVTLQR	6	Non-antigen	AYGGVLSS	H-2-Dd	0.4
	VTLQRGAAY	7	Non-antigen	F	H-2-Kd	0.41
	AYGGVLSSF	4	Non-antigen	SSFSGTVKY	H-2-Ld	0.58
	VLSSFSGTV	2	Non-antigen	KYNGSSYPF	H-2-Ld	Non-antigen
	LSSFSGTVK	1	Non-antigen	YPFPTTSET	H-2-Ld, H-2-	1.36
FimH	SSFSGTVKY	13	Non-antigen	TDKPWPVA	Dd, H-2-Kd	1.50
(46-128)	TVKYNGSSY	5	0.74	L	H-2-Kd	0.75
(10 120)	KYNGSSYPF	4	Non-antigen	KPWPVALY	H-2-Dd	Non-antigen
	SSYPFPTTS	1	Non-antigen	L	11 2 Du	rion unugen
	YPFPTTSET	4	0.58	L		
	TTSETPRVV	2	0.82	LYLTPVSSA		
	TSETPRVVY	5	0.76	VAIKAGSLI		
	ETPRVVYNS	1	Non-antigen	VAIIVAUSLI		
	TPRVVYNSR	1	Non-antigen			
	VVYNSRTDK	3	0.90			
	YNSRTDKPW	1	0.47			
	RTDKPWPVA	2				
		2	Non-antigen			
	TDKPWPVAL		Non-antigen			
	DKPWPVALY	1	0.49			
	KPWPVALYL	5	1.36			
	ALYLTPVSS	1	0.58			
	TPVSSAGGV	1	0.95			
	SSAGGVAIK	4	2.07			
	GVAIKAGSL	1	0.96			
	VAIKAGSLI	1	Non-antigen			
	AIKAGSLIA	1	Non-antigen			

Based on the findings from the Tepitool, 10 epitopes were predicted for 23 human MHC-II alleles, and four epitopes were identified for BALB/c H-2 class II alleles, specifically H2-IAd and H2-IEd for FimH. Regarding PapG II, seven epitopes were predicted for 17 human MHC II alleles, and one epitope for the mouse MHC-II H2-IEd. The selected human and mouse MHC-II epitopes are summarized in Table 3. Given the role of

T-cells in generating protective responses against UTIs caused by UPEC, the selected regions could increase the likelihood of inducing T-cell responses against UPEC.

Design of the final vaccine construct based on the immunodominant fragments

The final vaccine construct was made with one domain of PapG II (81 amino acids) and FimH (83

Table 3. MHC-II binding epitopes predicted by the TepiTool server with antigenicity score exceeding the threshold value

Protein	Epitope sequence	No. of human MHC-II alleles	Antigenicity (cut off ≥ 0.4)	Peptide Sequence	No. of mouse MHC-II alleles	Antigenicity
	YPLFIEVHNKGSWSE	6	0.53	FDDIIFKVALPADLP	H2-IEd	0.83
	EVHNKGSWSEENTGD	1	0.66			
	DSYFFLKGYKWDERA	3	Non-antigen			
PapG II	KGYKWDERAFDTANL	5	0.49			
	EKTRLTEKFDDIIFK	4	0.65			
	TEKFDDIIFKVALPA	4	0.76			
	DIIFKVALPADLPLG	5	0.70			
	DYPETITDYVTLQRG ITDYVTLQRGAAYGG	7 11	Non-antigen 0.48	PETITDYVTLQRGAA TPRVVYNSRTDKPWP	H2-IEd H2-IEd	
	LORGAAYGGVLSSFS	1	Non-antigen	WPVALYLTPVSSAGG	H2-IAd	
	AYGGVLSSFSGTVKY	2	Non-antigen	TPVSSAGGVAIKAGS	H2-IAd	
FimH	LSSFSGTVKYNGSSY	3	0.41			
	PFPTTSETPRVVYNS	2	0.44			
	SETPRVVYNSRTDKP	3	0.72			
	PVALYLTPVSSAGGV	3	0.91			
	LTPVSSAGGVAIKAG	5	1.06			
	SAGGVAIKAGSLIAV	1	1.00			

amino acids). The domains were joined together by a flexible linker sequence (GGGGSGGGGS). To enhance the immunogenicity of the vaccine construct, the N- (1-173) and C-terminal (401-495) conserved domains of FliC were placed at the beginning and end of the vaccine construct, respectively, using a rigid EAAAK linker. This linker was used to keep a fixed distance between the protein domains^[31]. Therefore, the vaccine construct was designed with 452 amino acid residues (Fig. S1).

Characterization of the vaccine construct

The vaccine sequence had a theoretical pI of 4.87, a molecular weight of 48.21 kDa, with an estimated half-life of >10 h for *E. coli*. The vaccine sequence also had an aliphatic index of 85.11, demonstrating significant thermostability. The instability index was 34.10, categorizing the sequence as stable (<40). Additionally, the vaccine sequence showed a negative GRAVY of -0.371. This negative GRAVY value indicates that the protein is non-polar and hydrophilic, making it likely to interact with water molecules. In addition, it had an antigenicity of 0.647 (greater than the threshold) and showed no allergenicity. According to the Protein-sol results, the vaccine was soluble, with a solubility score of 0.52 (greater than 0.45).

Secondary structure prediction of the recombinant protein

According to the data obtained from the GOR IV server, the final secondary structure of the vaccine consisted of 38.50% alpha helices, 15.04% beta sheets,

and 46.46% random coils. A graphical representation of the secondary structure features is shown in <u>Figure S2</u>.

Prediction of the tertiary structure, refinement, and validation

The 3D structure of the vaccine construct was predicted by the I-TASSER server. The model exhibiting the highest C-score was chosen as the optimal model (Fig. S3A). This 3D model was further refined using the GalaxyRefine web server, which generates five optimized 3D models. The best model (Fig. S3B) showed a GDTHA value of 0.9287, an RMSD value of 0.485, a MolProbity score of 2.163, and a Clash score of 28.7. The ProSA web tool also indicated that the overall quality Z-value of the optimized model was -8.14, which is considered high quality (Fig. S3C). Analysis of the Ramachandran plot of the refined model revealed that 89.8% of the residues were located in the most favored regions, 7.2% in the additional allowed regions, 1% in the generously allowed regions, and 2% in the disallowed regions (Fig. S3D).

Analysis of molecular docking interactions

To characterize the binding affinity of the vaccine construct for human TLRs, we utilized ClusPro 2.0 for molecular docking. For each docking, the server generated a total of 30 clusters, and the cluster with the lowest energy score was considered the result. The lowest energy scores of the vaccine construct-TLR-5 and vaccine construct-TLR-4 docking complexes were predicted to be -1164.5 and -981.1, respectively.

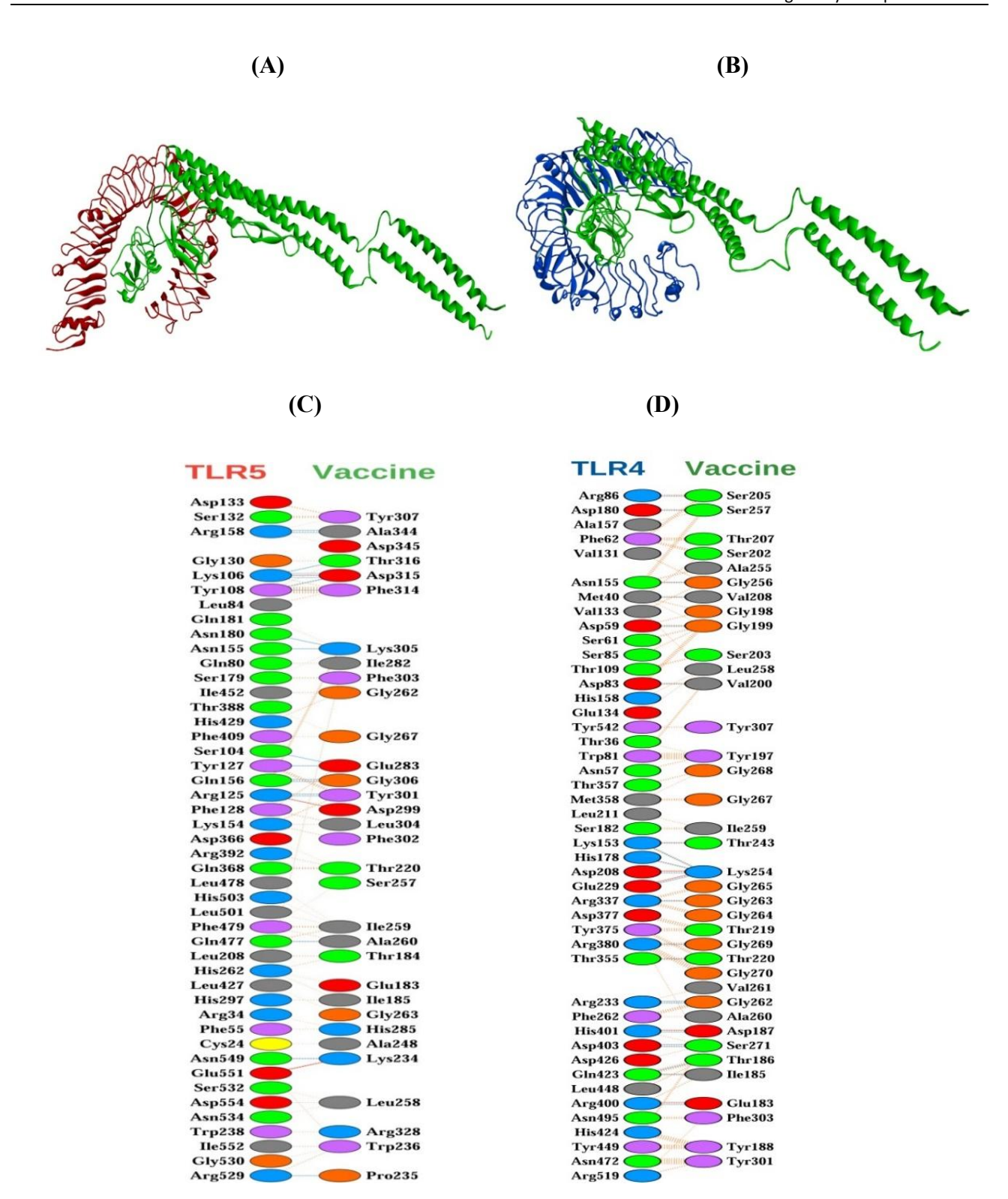


Fig. 1. Analysis of the vaccine construct with TLRs. (A) The best-docked complex of the vaccine construct with TLR-5 showed a binding energy of -1164.5. The vaccine construct is shown in green color, while the TLR-5 receptor is in red color. (B) The best-docked complex of the vaccine construct with TLR-4 indicated a binding energy of 981.1. The vaccine construct is depicted in green color, while TLR-5 receptor is in blue color. (C) The vaccine construct-TLR-5 complex was analyzed for interactions and 2D images were taken. (D) The vaccine construct-TLR-4 complex was analyzed for interactions and the 2D images were taken (red: salt bridges, yellow: disulfide bond, blue: hydrogen bond, and orange: non-bonded contacts).

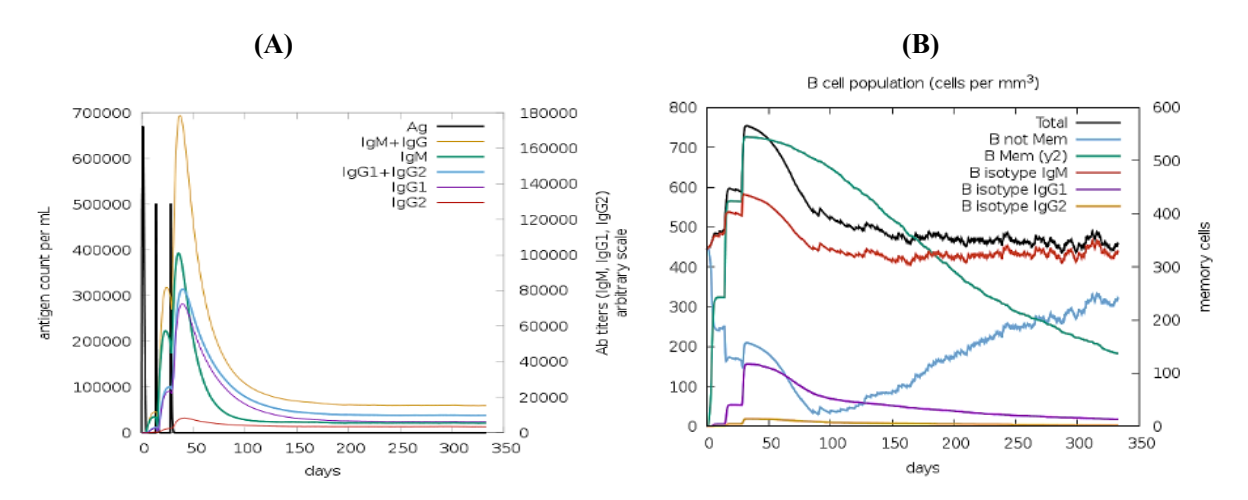


Fig. 2. In silico immune response simulations of the vaccine construct. (A) Simulation of antibody response upon antigen exposure, showing rapid antigen clearance and robust production of IgM, IgG, and their subclasses following vaccination. (B) Simulation of B-cell population, B-cell population dynamics, including total B-cells, memory B-cells, and isotype-specific responses (IgM, IgG1, and IgG2), indicating effective induction of memory and isotype switching.

According to the PRODIGY results, the vaccine construct exhibited the strongest affinity toward TLR-5 (ΔG =-21.1 kcal/mol) with Kd (M) at 25.0°C: 3.4E-16. Strongest affinity toward TLR-4 (ΔG = -16.2 kcal/mol with Kd (M) at 25.0°C: 1.3E-12 confirmed the high-affinity binding patterns between the vaccine construct and TLRs. The molecular docking results for vaccine construct interacting with TLR-5 and TLR-4 were visualized using the Discovery Studio visualizer (Fig. 1A and 1B). The PDBSum analysis showed that 46 residues of TLR-5 (chain A) interacted with 32

residues of the vaccine construct (chain B). This interaction included 3 salt bridges, 18 hydrogen bonds, and 297 non-bonded contacts (Fig. 1C). The results of docking of the vaccine construct with TLR-4 showed that the number of interface residues of the vaccine construct and TLR-4 was 37 and 45, respectively. A total of 4 salt bridges, 22 hydrogen bonds, and 260 non-bonded contacts were found in the vaccine construct-TLR-4 complex (Fig. 1D). Overall, these results indicate that the designed vaccine construct exhibits a strong binding affinity for both TLR-4 and TLR-5.

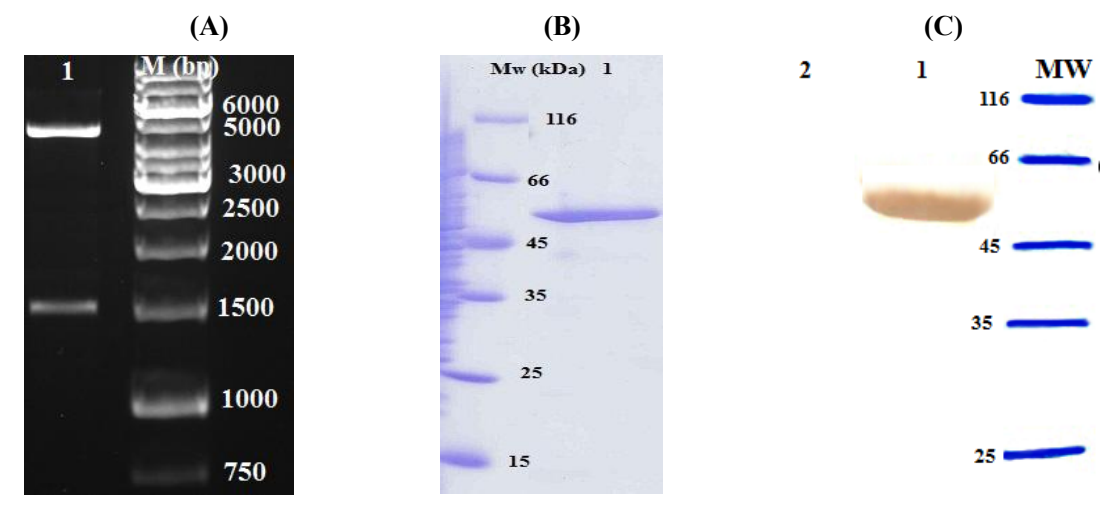


Fig. 3. Cloning of the gene and purification of the recombinant protein. (A) Confirmation of gene cloning by enzyme digestion (lane 1: digested recombinant plasmid and M; Molecular weight marker), (B) evaluation of the purified protein by SDS-PAGE (lane 1: elution 1 of the purified protein), (C) confirmation of the purified protein by Western blot analysis (Lane 1: elution 1 of the purified protein and lane 2: un-induced clone). Mw: Un-stained protein marker.

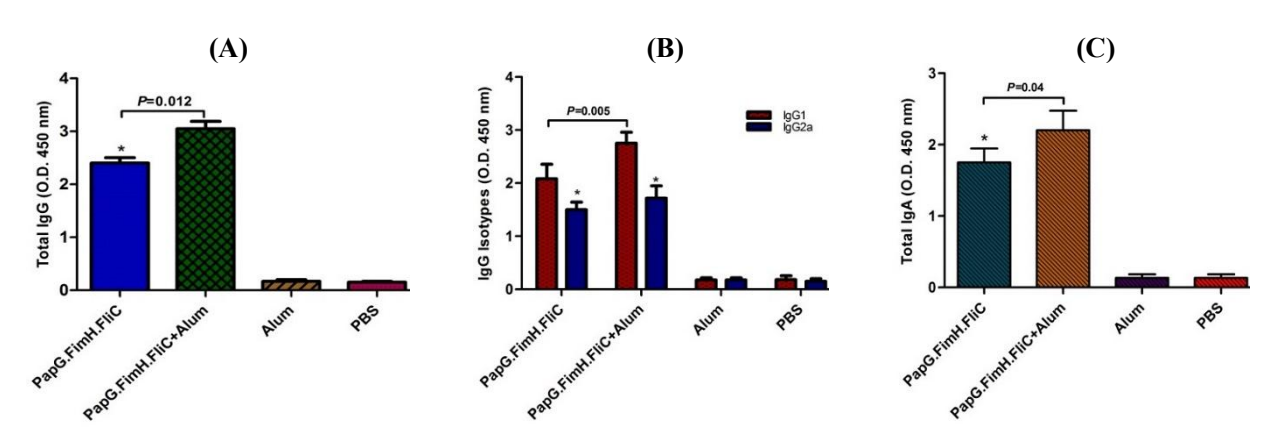


Fig. 4. Evaluation of systemic antibody responses. BALB/c mice were injected with different vaccine formulations, including PapG/FimH/FliC alone and PapG/FimH/FliC combined with alum. Control groups received alum and PBS. Blood samples were collected two weeks after the last vaccine dose. The levels of (A) total IgG, (B) IgG isotypes, and (C) IgA responses in the vaccinated groups were measured by ELISA. The results represent the mean values (\pm SD) of three repeated experiments at serum dilution of 1:100. The difference between PapG/FimH/FliC and PapG/FimH/FliC combined with alum in inducing humoral responses is indicated by brackets with p value. * Statistical significance of total IgG, IgG1, and IgG2a over control groups (p < 0.05).

Simulation of the Host's immune response

An in silico simulation of the immune response was performed to confirm the ability of the vaccine construct to induce an immune response. The vaccine construct demonstrated robust immune activity across primary, secondary, and tertiary immune responses, followed by the time steps of injection. As shown in Fig. 2A, production antibody began after the immunization. All the antibody types peaked after the secondary and tertiary vaccine exposure. The highest antibody titer was related to IgM+IgG, followed by IgM alone, IgG1+IgG2, IgG1, and IgG2, indicating a progression in immune response. In addition, an increase in the population of memory B-cells was observed (Fig. 2B).

Expression and purification of the recombinant protein

The synthesized and codon-optimized gene construct was cloned into the pET28a vector. After transformation and culture on LB agar, the recombinant plasmids containing the gene construct were confirmed by enzyme digestion (Fig. 3A) and then sequenced (data not shown). SDS-PAGE analysis showed protein expression after adding 1 mM of IPTG and a 5 h incubation time period (data not shown). The expression of the induced protein was further confirmed by Western blot analysis using a monoclonal antibody. The recombinant protein was successfully purified using Ni-NTA affinity chromatography, with its purity and concentration confirmed by SDS-PAGE and Western blotting (Fig. 3B and 3C). The size of the purified protein was approximately 53 kDa. After applying the LPS removal column, the LPS concentration reached less than 1 EU/ml, as determined by the LAL assay. The

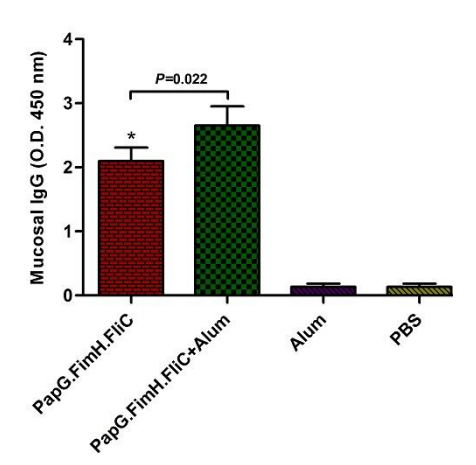
concentration of the dialyzed and purified protein was measured at 500 μ g/ml using the BCA assay kit.

Responses of serum antibody

To investigate the immune responses elicited by the vaccine candidate, we administered different vaccine formulations to mice and measured the induced responses. Serum samples were collected two weeks after the last immunization and analyzed for levels of antigen-specific IgG, IgG isotypes, and IgA antibodies using ELISA. The results showed significantly increased levels of serum IgG, IgG isotypes, and IgA antibodies in the PapG/FimH/FliC group after the third vaccine dose, as compared to the control groups (p <0.05; Fig. 4). Additionally, we observed that when alum was added to PapG/FimH/FliC, the levels of total IgG, IgG1, and IgA responses significantly increased compared to the mice that received PapG/FimH/FliC alone (p < 0.05). However, there was no significant difference in the IgG2a response between the mice that received PapG/FimH/FliC and PapG/FimH/FliC in combination with alum (p > 0.05).

Responses of mucosal antibody

To further confirm the production of IgG and IgA in mucosal fluids, we measured the levels of anti-PapG/FimH/FliC IgA and IgG in urine samples collected after the third immunization. The findings that immunization of revealed mice PapG/FimH/FliC significantly elicited both IgG and IgA levels in the urine samples compared to the control groups (p < 0.05; Fig. 5). Also, we observed that the addition of alum to the recombinant protein could significantly induce the mucosal IgG responses more than PapG/FimH/FliC without alum (p = 0.022; Fig. 5B).



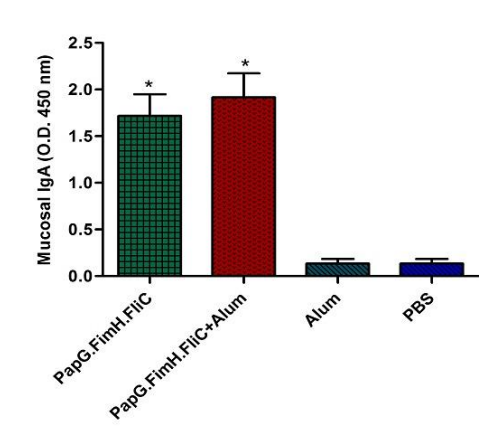


Fig. 5. Evaluation of mucosal antibody responses in the urine. After the last vaccine dose, (A) IgG and (B) IgA levels were measured in the urine samples collected from the immunized mice. The results represent the mean values (\pm SD) of three-repeated experiments. Statistical analysis was performed using one-way ANOVA or student's t-test, with the p value indicating significant differences. * Statistical significance of antibodies levels compared to the control groups (p < 0.05).

DISCUSSION

UTIs are common bacterial infections that affect approximately 150 million people worldwide each year, resulting in significant social costs^[32]. Certain types of UTIs, such as recurrent UTIs, pyelonephritis, and urosepsis, can be life-threatening and difficult to manage^[1]. Various vaccine strategies have been developed to combat UTIs; however, none of them have successfully produced a universal and safe vaccine for UTIs ^[33]. Research has focused on evaluating the efficacy of key VFs of UTI pathogens, especially UPEC strains. These vaccine targets have been designed in different forms, including single, fusion, and multiepitope, with some progressing to clinical trials^[34].

Effective defense against UTIs requires a broad immune response that engages both innate and adaptive immune mechanisms. Immunoinformatic approaches can help design vaccines that activate all aspects of the immune system by identifying immunodominant B- and T-cell epitopes within candidate antigens. Using immunoinformatic methods for vaccine development is highly desirable due to their safety, cost-effectiveness, and high efficiency^[35]. However, recombinant multiepitope vaccines face challenges, including low immune response and dominant reactions to junctional epitopes. To address these limitations, the use of effective adjuvants and linkers is suggested^[36].

P fimbriae are recognized as one of the most common VFs of UPEC in the pathogenesis of UTIs, especially pyelonephritis^[32]. Research by Kudinha and Kong has demonstrated that specific alleles of the PapG adhesion, including PapG II, are strongly associated with pyelonephritis^[37]. A recent study has evaluated a vaccine candidate based on the PapA subunit from P

fimbriae; however, the results were not promising^[32]. Another study had reported that a vaccine candidate containing PapDG successfully protected cynomolgus monkeys from pyelonephritis infection^[38-40].

FimH, a component of type 1 fimbriae, has emerged as a promising vaccine target for UTIs caused by UPEC, especially in cases of recurrent UTIs. Clinical trials of a FimH-based vaccine candidate have demonstrated that vaccination of mice and monkeys with FimH reduces bladder colonization. In addition, treatment with anti-FimH IgG has been found to decrease UPEC colonization in the bladders of patients experiencing recurrent UTIs^[41,42]. Given the roles of type 1 and P fimbriae in UPEC colonization of the bladder and kidneys, as well as the potential synergistic effect between FimH and PapG II in contributing to pyelonephritis, a vaccine that combines both FimH and PapG II may be more effective in preventing bladder and kidney infections compared to the vaccines that target either protein alone^[43].

The FliC from bacteria such as *S. typhimurium* has been studied as an adjuvant, with some flagellin-based vaccines entering clinical trials. For instance, a flagellin-adjuvanted influenza vaccine has shown promising results in phase I/II clinical trials^[44]. Predictions from ProsA and Ramachandran plots indicate that the designed vaccine construct exhibits desirable properties. The chimeric protein PapG/FimH/FliC indicated essential properties of an ideal vaccine candidate, especially the presence of B-cell epitopes and T-cell binding peptides for MHC-I and MHC-II, which stimulate both humoral and cellular immune responses.

Our animal studies revealed that subcutaneous vaccination of mice with the chimeric protein, without the use of alum adjuvant, not only induced systemic

immune responses in serum but also induced mucosal immune responses in the urine. Because the PapG/FimH without FliC, and FliC alone groups were not included in the study, making it challenging to definitely elucidate the specific role of FliC as an innate adjuvant. Additional experiments are required to confirm the role of FliC as an adjuvant in this vaccine formulation. Moreover, similar to other studies, the possible adjuvant effect of FimH in the vaccine construct may significantly contribute to the elevated systemic and mucosal humoral responses^[5,6].

Th1 responses are associated with the production of IgG2a, while Th2 responses are characterized by increased levels of IgG1 antibodies. In our study, mice immunized with the vaccine construct exhibited higher levels of IgG1 (Th2) compared to IgG2a (Th1) antibodies. This observation suggests that the vaccine formulation tends to promote an antibody-mediated immune response. Previous studies have reported that FliC can induce both Th1 and Th2 responses, with evidence showing a preference for shifting responses toward Th2 (humoral response)^[45-47]. Additionally, the inclusion of alum adjuvant in our study enhanced the production of IgG1 (Th2) antibodies against the vaccine construct. To further assess the Th1/Th2 profile among the immunized mice, we measured the ratio of IgG1 to IgG2a. The results showed that alum increased the IgG1/IgG2a ratio and switched the immune responses toward Th2. These results were in accordance with the other studies which have reported alum as a stimulator of Th2-type responses^[48,49]. Supporting our findings, Habibi and colleagues have demonstrated that adding alum to the FyuA antigen from a UPEC strain enhances both IgG1 and IgG2a responses, with IgG1 levels exceeding those of IgG2a^[50].

CONCLUSION

In the present study, a chimeric protein was designed by incorporating key domains of the FimH and PapG II proteins of UPEC and incorporating the most promising B- and T-cell epitopes. In addition, the conserved N- and C-terminal domains of FliC from *S. typhimurium* were included in the vaccine construct. Bioinformatics and immunoinformatics analyses confirmed the quality of the vaccine construct. In silico simulations of the immune response showed elevated levels of B-cells. Furthermore, the chimeric protein showed stable interactions with TLR-4 and TLR-5, suggesting its potential to activate innate immune responses. The vaccine construct induced significant levels of systemic IgG, IgG isotypes and IgA, along with mucosal antibody responses in mice. The inclusion of alum adjuvant

significantly enhanced systemic IgG1 and mucosal IgG levels compared to the non-adjuvanted construct. Ongoing experiments are evaluating the cellular immune responses and the protective efficacy of the vaccine formulations in a mouse model.

DECLARATIONS

Acknowledgments

The authors would like to acknowledge the staff at the Department of Molecular Biology of the Pasteur Institute of Iran for their assistance and support of this research project. It is also mentioned that artificial intelligence (AI) has not used in the preparation of the manuscript.

Ethical approval

All the animal experiments were conducted in accordance with the Institutional Animal Care guidelines and approved by Shahr-e-Qods Branch, Islamic Azad University, Tehran, Iran (ethical code: IR.IAU.QODS.REC.1402.010).

Consent to participate

Not applicable.

Consent for publication

All authors reviewed the results and approved the final version of the manuscript.

Authors' contributions

SM: Writing-original draft, methodology, investigation, Data curation, and conceptualization; Software, methodology, Data investigation, review and editing; TR: Investigation, conceptualization, Data curation, review and editing; FF: Review and editing, project administration, investigation, resources, validation, conceptualization; MRAK: Review and editing, project administration, methodology, investigation, resources, validation, funding acquisition, and conceptualization.

Data availability

All relevant data can be found within the manuscript.

Competing interests

The authors declare that they have no competing interests.

Funding

This work was supported by the Pasteur Institute of Iran.

REFERENCES

- Mancuso G, Midiri A, Gerace E, Marra M, Zummo S, Biondo C. Urinary Tract Infections: The Current Scenario and Future Prospects. Pathogens. 2023;12(4).
- Nielubowicz GR, Mobley HLT. Host-pathogen interactions in urinary tract infection. Nature Reviews Urology. 2010;7(8):430-41.
- Mobley HL, Jarvis KG, Elwood JP, Whittle DI, Lockatell CV, Russell RG, et al. Isogenic P-fimbrial deletion mutants of pyelonephritogenic Escherichia coli: the role of α Gal (1–4) β Gal binding in virulence of a wild-type strain. Molecular microbiology. 1993;10(1):143-55.
- 4. Zhou Y, Zhou Z, Zheng L, Gong Z, Li Y, Jin Y, et al. Urinary Tract Infections Caused by Uropathogenic Escherichia coli: Mechanisms of Infection and Treatment Options. International Journal of Molecular Sciences. 2023;24(13):10537.
- Ashkar AA, Mossman KL, Coombes BK, Gyles CL, Mackenzie R. FimH adhesin of type 1 fimbriae is a potent inducer of innate antimicrobial responses which requires TLR4 and type 1 interferon signalling. PLoS Pathog. 2008;4(12):e1000233.
- Mian MF, Lauzon NM, Andrews DW, Lichty BD, Ashkar AA. FimH can directly activate human and murine natural killer cells via TLR4. Mol Ther. 2010;18(7):1379-88.
- Facciolà A, Visalli G, Laganà A, Di Pietro A. An overview of vaccine adjuvants: current evidence and future perspectives. Vaccines. 2022;10(5):819.
- 8. Zhao T, Cai Y, Jiang Y, He X, Wei Y, Yu Y, et al. Vaccine adjuvants: mechanisms and platforms. Signal Transduction and Targeted Therapy. 2023;8(1):283.
- 9. Hajam IA, Dar PA, Shahnawaz I, Jaume JC, Lee JH. Bacterial flagellin—a potent immunomodulatory agent. Experimental & Molecular Medicine. 2017;49(9):e373-e.
- 10. Melican K, Sandoval RM, Kader A, Josefsson L, Tanner GA, Molitoris BA, et al. Uropathogenic Escherichia coli P and Type 1 fimbriae act in synergy in a living host to facilitate renal colonization leading to nephron obstruction. PLoS Pathog. 2011;7(2):e1001298.
- 11. Apweiler R, Bairoch A, Wu CH, Barker WC, Boeckmann B, Ferro S, et al. UniProt: the universal protein knowledgebase. Nucleic acids research. 2004;32(suppl 1):D115-D9.
- 12. Krammer E-M, Bridot C, Serna S, Echeverria B, Semwal S, Roubinet B, et al. Structural insights into a cooperative switch between one and two FimH bacterial adhesins binding pauci- and high-mannose type N-glycan receptors. Journal of Biological Chemistry. 2023;299(5):104627.
- 13. Lane M, Mobley H. Role of P-fimbrial-mediated adherence in pyelonephritis and persistence of uropathogenic Escherichia coli (UPEC) in the mammalian kidney. Kidney international. 2007;72(1):19-25.
- 14. Doytchinova IA, Flower DR. VaxiJen: a server for prediction of protective antigens, tumour antigens and subunit vaccines. BMC bioinformatics. 2007;8(1):4.

- Paul S, Sidney J, Sette A, Peters B. TepiTool: A Pipeline for Computational Prediction of T Cell Epitope Candidates. Curr Protoc Immunol. 2016;114:18.9.1-.9.24.
- Gasteiger E, Gattiker A, Hoogland C, Ivanyi I, Appel RD, Bairoch A. ExPASy: The proteomics server for in-depth protein knowledge and analysis. Nucleic Acids Res. 2003;31(13):3784-8.
- 17. Dimitrov I, Flower DR, Doytchinova I, editors. AllerTOP-a server for in silico prediction of allergens. BMC bioinformatics; 2013: Springer.
- 18. Gupta S, Kapoor P, Chaudhary K, Gautam A, Kumar R, Consortium OSDD, et al. In silico approach for predicting toxicity of peptides and proteins. PloS one. 2013;8(9):e73957.
- 19. Hebditch M, Carballo-Amador MA, Charonis S, Curtis R, Warwicker J. Protein–Sol: a web tool for predicting protein solubility from sequence. Bioinformatics. 2017;33(19):3098-100.
- Garnier J. GOR secondary structure prediction method version IV. Meth Enzym, RF Doolittle Ed. 1998;266:540-53.
- 21. Roy A, Kucukural A, Zhang Y. I-TASSER: a unified platform for automated protein structure and function prediction. Nature protocols. 2010;5(4):725-38.
- 22. Ko J, Park H, Heo L, Seok C. GalaxyWEB server for protein structure prediction and refinement. Nucleic acids research. 2012;40(W1):W294-W7.
- 23. Wiederstein M, Sippl MJ. ProSA-web: interactive web service for the recognition of errors in three-dimensional structures of proteins. Nucl Acids Res. 2007;35(suppl 2):W407-W10.
- Laskowski RA, MacArthur MW, Moss DS, Thornton JM. PROCHECK: a program to check the stereochemical quality of protein structures. J Appl Crystallogr. 1993;26(2):283-91.
- 25. Kozakov D, Hall DR, Xia B, Porter KA, Padhorny D, Yueh C, et al. The ClusPro web server for protein—protein docking. Nature protocols. 2017;12(2):255-78.
- 26. Xue LC, Rodrigues JP, Kastritis PL, Bonvin AM, Vangone A. PRODIGY: a web server for predicting the binding affinity of protein–protein complexes. Bioinformatics. 2016;32(23):3676-8.
- Laskowski RA. PDBsum: summaries and analyses of PDB structures. Nucleic acids research. 2001;29(1):221-
- 28. Rapin N, Lund O, Bernaschi M, Castiglione F. Computational immunology meets bioinformatics: the use of prediction tools for molecular binding in the simulation of the immune system. PloS one. 2010;5(4):e9862.
- 29. Karam MRA, Rezaei AA, Siadat SD, Habibi M, Bouzari S. Evaluation of prevalence, homology and immunogenicity of dispersin among enteroaggregative Escherichia coli isolates from Iran. Iranian biomedical journal. 2017;21(1):40.
- 30. Shahbazi S, Badmasti F, Habibi M, Sabzi S, Goodarzi NN, Farokhi M, et al. In silico and in vivo Investigations of the Immunoreactivity of Klebsiella pneumoniae OmpA Protein as a Vaccine Candidate. Iranian

- biomedical journal. 2024;28(4):156.
- 31. Chen X, Zaro JL, Shen WC. Fusion protein linkers: property, design and functionality. Adv Drug Deliv Rev. 2013;65(10):1357-69.
- 32. Gupta S, Kumar P, Rathi B, Verma V, Dhanda RS, Devi P, et al. Targeting of Uropathogenic Escherichia coli papG gene using CRISPR-dot nanocomplex reduced virulence of UPEC. Scientific reports. 2021;11(1):17801.
- 33. Dhakal B, Kulesus R, Mulvey M. Mechanisms and consequences of bladder cell invasion by uropathogenic Escherichia coli. European journal of clinical investigation. 2008;38:2-11.
- Karam MRA, Habibi M, Bouzari S. Urinary tract infection: Pathogenicity, antibiotic resistance and development of effective vaccines against Uropathogenic Escherichia coli. Molecular immunology. 2019;108:56-67.
- 35. Saldanha L, Langel Ü, Vale N. In Silico Studies to Support Vaccine Development. Pharmaceutics. 2023;15(2):654.
- 36. Khalid K, Poh CL. The Promising Potential of Reverse Vaccinology-Based Next-Generation Vaccine Development over Conventional Vaccines against Antibiotic-Resistant Bacteria. Vaccines. 2023;11(7):1264.
- 37. Kudinha T, Kong F. Distribution of papG alleles among uropathogenic Escherichia coli from reproductive age women. Journal of biomedical science. 2022;29(1):66.
- 38. Jinek M, Chylinski K, Fonfara I, Hauer M, Doudna JA, Charpentier E. A programmable dual-RNA-guided DNA endonuclease in adaptive bacterial immunity. Science. 2012;337(6096):816-21.
- 39. Roberts JA, Kaack MB, Baskin G, Chapman MR, Hunstad DA, Pinkner JS, et al. Antibody responses and protection from pyelonephritis following vaccination with purified Escherichia coli PapDG protein. The Journal of urology. 2004;171(4):1682-5.
- 40. O'brien VP, Hannan TJ, Nielsen HV, Hultgren SJ. Drug and vaccine development for the treatment and prevention of urinary tract infections. Urinary tract infections: Molecular pathogenesis and clinical management. 2017:589-646.
- 41. Eldridge GR, Hughey H, Rosenberger L, Martin SM, Shapiro AM, D'Antonio E, et al. Safety and immunogenicity of an adjuvanted Escherichia coli adhesin vaccine in healthy women with and without histories of recurrent urinary tract infections: results from

- a first-in-human phase 1 study. Human vaccines & immunotherapeutics. 2021;17(5):1262-70.
- 42. Starks CM, Miller MM, Broglie PM, Cubbison J, Martin SM, Eldridge GR. Optimization and qualification of an assay that demonstrates that a FimH vaccine induces functional antibody responses in women with histories of urinary tract infections. Human vaccines & immunotherapeutics. 2021;17(1):283-92.
- 43. Tseng C-C, Lin W-H, Wu A-B, Wang M-C, Teng C-H, Wu J-J. Escherichia coli FimH adhesins act synergistically with PapGII adhesins for enhancing establishment and maintenance of kidney infection. Journal of Microbiology, Immunology and Infection. 2022;55(1):44-50.
- Rhee JH, Khim K, Puth S, Choi Y, Lee SE. Deimmunization of flagellin adjuvant for clinical application. Current opinion in virology. 2023;60:101330.
- 45. Huleatt JW, Jacobs AR, Tang J, Desai P, Kopp EB, Huang Y, et al. Vaccination with recombinant fusion proteins incorporating Toll-like receptor ligands induces rapid cellular and humoral immunity. Vaccine. 2007;25(4):763-75.
- 46. Bargieri DY, Rosa DS, Braga CJ, Carvalho BO, Costa FT, Espíndola NM, et al. New malaria vaccine candidates based on the Plasmodium vivax Merozoite Surface Protein-1 and the TLR-5 agonist Salmonella Typhimurium FliC flagellin. Vaccine. 2008;26(48):6132-42.
- 47. McSorley SJ, Ehst BD, Yu Y, Gewirtz AT. Bacterial flagellin is an effective adjuvant for CD4+ T cells in vivo. The Journal of Immunology. 2002;169(7):3914-9.
- 48. Laera D, HogenEsch H, O'Hagan DT. Aluminum adjuvants—'Back to the Future'. Pharmaceutics. 2023;15(7):1884.
- 49. Su Z, Boucetta H, Shao J, Huang J, Wang R, Shen A, et al. Next-generation aluminum adjuvants: immunomodulatory layered double hydroxides NanoAlum reengineered from first-line drugs. Acta Pharmaceutica Sinica B. 2024.
- Habibi M, Karam MRA, Bouzari S. Evaluation of prevalence, immunogenicity and efficacy of FyuA iron receptor in uropathogenic Escherichia coli isolates as a vaccine target against urinary tract infection. Microbial Pathogenesis. 2017;110:477-83.